Available online at www.sciencedirect.com
ScienceDirect
Journal of Power Sources 173 (2007) 606–612
JOURNAL OF POWER SOURCES
www.elsevier.com/locate/jpowsour

Electrochemical capacitance of NiO/$Ru_{0.35}V_{0.65}O_2$ asymmetric electrochemical capacitor

Chang-Zhou Yuan, Bo Gao, Xiao-Gang Zhang *

College of Material Science & Engineering, Nanjing University of Aeronautics and Astronautics, Nanjing 210016, PR China

Received 12 December 2006; received in revised form 20 March 2007; accepted 18 April 2007
Available online 24 April 2007

Abstract

A designed asymmetric hybrid electrochemical capacitor was presented where NiO and $Ru_{0.35}V_{0.65}O_2$ as the positive and negative electrode, respectively, both stored charge through reversible faradic pseudocapacitive reactions of the anions (OH^-) with electroactive materials. And the two electrodes had been individually tested in 1 M KOH aqueous electrolyte to define the adequate balance of the active materials in the hybrid system as well as the working voltage of the capacitor based on them. The electrochemical tests demonstrated that the maximum specific capacitance and energy density of the asymmetric hybrid electrochemical capacitor were 102.6 F g^{-1} and 41.2 Wh kg^{-1}, respectively, delivered at a current density of 7.5 A cm^{-2}. And the specific energy density decreased to 23.0 Wh kg^{-1} when the specific power density increased up to 1416.7 W kg^{-1}. The hybrid electrochemical capacitor also exhibited a good electrochemical stability with 83.5% of the initial capacitance over consecutive 1500 cycle numbers.

Keywords: $Ru_{0.35}V_{0.65}O_2$; NiO; Hybrid electrochemical capacitor

1. Introduction

Electrochemical capacitors (ECs) have been recently attracting considerable attention due to their large specific capacitance (SC) and potential applications in hybrid vehicles and memory back-up systems [1]. Even though ECs can meet the power goal without difficulty, the lower energy density of ECs, in comparison with secondary battery, is the greatest drawback for some specific devices, such as electric vehicle (EV) applications, etc. [1]. In view of practical applications, attempts should be addressed to the improvement of energy density for ECs. And moreover, it is well established [2] that the promising routes to get around the problem of energy density of an EC are to maximize its capacitance by adopting the electrode materials with large SC, and to widen electrochemical window through the choice of a certain hybrid system based on different electrode materials.

Due to the low utilization of the carbon-based material [3] and degradation of the conducting polymer material [4,5], substantial researches have been targeted to the excellent electrode material, Ruthenium oxide [6] with remarkable large SC ranging from 720 to 760 F g^{-1}. However, the high cost has necessitated the need to reduce the amount of Ru species and to utilize ruthenium oxide efficiently by the addition of the second metal oxide, such as TiO_2, VO_x, MoO_3, etc., [7–9], or to identify low cost and benign alternative transition metal oxides such as NiO [10], etc.

Recently, the hybrid EC, regarded as a new trend in ECs, has been reported greatly [11–17]. The new type hybrid asymmetric ECs are distinguished from either electrical double-layer capacitors (EDLCs) or the conventional batteries. Such hybrid ECs are always assembled with positive electrode with the large positive cutoff potential and negative electrode with high hydrogen overpotential, which results in a significant increase of the overall cell operating voltage and energy density of ECs. So it is possible to obtain the desired large electrochemical window and specific energy density of an EC by means of choosing some proper electroactive materials as positive and negative electrodes, respectively. Additionally, the case studied commonly is that one electrode is storing charge through a reversible non-faradic process of ionic movement on the surface of an activated carbon or the hole of nano-pore carbon materials, and the other

* Corresponding author. Tel.: +86 25 52112902; fax: +86 25 52112626.
E-mail address: azhangxg@163.com (X.-G. Zhang).

0378-7753/$ – see front matter © 2007 Elsevier B.V. All rights reserved.
doi:10.1016/j.jpowsour.2007.04.034

is to utilize reversible faradic redox reactions of metal oxides [11–16]. It is rarely studied that both of the positive and negative electrodes of an asymmetric EC are based on metal oxides [17], on which different faradic redox processes take place reversibly.

Based on the above viewpoints, in this paper, we present a new concept of hybrid EC, in which $Ru_{0.36}V_{0.64}O_2$ negative electrode with a high hydrogen evolution overpotential which enables a large negative cutoff potential is in combination with the NiO positive electrode, in 1 M KOH electrolyte solution. The electrochemical capacitance performance of the hybrid EC was evaluated by means of cyclic voltammetry (CV), galvanostatic charge–discharge and electrochemical impedance spectroscopy (EIS) techniques. All the electrochemical tests demonstrated that the hybrid EC owned good electrochemical capacitance performance.

2. Experimental

2.1. Preparation of electrode materials

NiO was synthesized in the ethanol–water system (EWS) and then calcinated at 300 °C as follows. Firstly, a certain amount of $Ni(NO_3)_2{\cdot}6H_2O$ was dissolved in absolute ethanol to form a green homogeneous solution (0.018 M). Three hour later, the pH of the solution was slowly adjusted to 9 by dropwise addition of 0.025 M NaOH at room temperature. The resulting suspension was stirred at the same temperature for 6 h. Thus, the mixture was aged for another 6 h and then filtered, washed with copious absolute ethanol, dried at 40 °C in air for 24 h and then calcinated at 300 °C for 1.5 h. Black NiO was obtained.

As for the synthesis of $Ru_{0.36}V_{0.64}O_2$, the vanadium sol should be prepared in advance, and the method employed for the synthesis of the vanadium sol was the same as described in the reference [18], except where otherwise indicated. V_2O_5 powder (1 g) was dissolved completely in an ice-cooled 30% H_2O_2 (50 ml), to yield a bright reddish brown solution. A vigorous oxygen evolution generated by decomposition of excess H_2O_2 occurred in 20–25 min with stirring all the time. Meanwhile, the solution turned to a dark brown sol with a considerable viscosity. As-prepared sol was diluted with acetone and water orderly at a volume fraction of 1:1:1. Then some certain amount of $RuCl_3{\cdot}xH_2O$ was added into the sol according to Ru/V ratio of 9:16 in atom and continually stirred for 48 h. The black product of the reaction was washed with abundant distilled water and absolute ethanol, dried at 65 °C and then calcinated at 400 °C for 4 h. Thus, $Ru_{0.36}V_{0.64}O_2$ was synthesized.

The prepared samples were characterized by means of XRD (Max 18 XCE Japan), using a Cu Ka source and energy-dispersive analysis by X-ray (EDAX, Link-200, Britain).

2.2. Electrochemical tests

The NiO electrode was prepared as follows. The mixture containing 75 wt.% as-prepared NiO and 20 wt.% acetyleneblack (AB) and 5 wt.% polytetrafluoroethylene (PTFE) was well mixed and pressed (1.2×10^7 Pa) onto a nickel grid served as a current collector (surface area is 1 cm^2). The $Ru_{0.36}V_{0.64}O_2$ electrode was prepared by the same method as that of the positive electrode described above and composed of 60 wt.% $Ru_{0.36}V_{0.64}O_2$, 35 wt.% AB and 5 wt.% PTFE. The typical mass loadings of positive electrode material (NiO) and negative electrode material ($Ru_{0.36}V_{0.64}O_2$) were 10 and 5 mg, respectively.

A beaker-type electrochemical cell was used for the electrochemical measurement of NiO and $Ru_{0.36}V_{0.64}O_2$ electrodes, individually, in 1 M KOH electrolyte. The cell was equipped with a working electrode, a platinum plate counter electrode and a saturated calomel electrode (SCE) as reference electrode.

Cyclic voltammetry (CV) and EIS measurements were performed by using CHI 660 electrochemical workstation. The galvanostatic charge/discharge performance of both two electrodes and the hybrid EC was evaluated with an Arbin BT2042 battery workstation system in a certain range of potentials.

3. Results and discussion

3.1. The characteristics of NiO and $Ru_{0.36}V_{0.64}O_2$

The XRD pattern of the as-prepared NiO is presented in Fig. 1a, and the characteristic reflections at (1 1 1), (2 0 0), (2 2 0), (3 1 1) and (2 2 2) show that as-prepared NiO has a rhombohedral

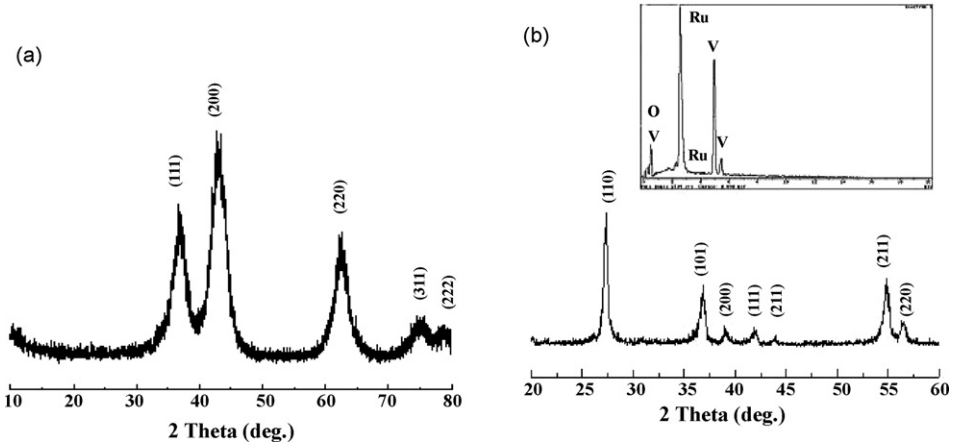

Fig. 1. The XRD patterns of (a) NiO and (b) $Ru_{0.36}V_{0.64}O_2$, and EDAX of $Ru_{0.36}V_{0.64}O_2$ (inset).

crystalline structure (Joint Committee on Powder Diffraction standards (JCPDS) Powder Diffraction File Card No. 44-1159). The broadening of the X-ray diffraction lines is suggestive of the fine size of the synthesized NiO. The crystallite size of NiO, in the direction perpendicular to the major diffraction peak (2 0 0) ($2\theta = 43.26^\circ$), can be estimated as ca. 5 nm from the XRD lines using the Scherer's formula. Fig. 1b shows the X-ray diffraction pattern of $Ru_{0.36}V_{0.64}O_2$. The characteristic peaks at 27.32°, 36.88°, 39.08°, 41.12°, 44.00°, 54.86° and 56.28° 2θ are corresponding to (1 1 0), (1 0 1), (2 0 0), (1 1 1), (2 1 0), (2 1 1) and (2 2 0) planes, respectively, which matches well with the report in reference [19,20]. The energy dispersive X-ray analysis (EDAX) pattern of $Ru_{0.36}V_{0.64}O_2$, shown in the inset picture in Fig. 1b, reveals the presence of V species incorporated into the ruthenium oxide and demonstrates that the EDAX determination of ratio of Ru/V in $Ru_{0.36}V_{0.64}O_2$ binary oxide is basically in line with that added previously.

3.2. Electrochemical behaviors of NiO and $Ru_{0.36}V_{0.64}O_2$ electrodes

CV was firstly applied to detect the electrochemical window and electrochemical reaction reversibility of $Ru_{0.36}V_{0.64}O_2$ electrode in 1 M KOH electrolyte solution. Fig. 2a shows typical *E–i* response of $Ru_{0.36}V_{0.64}O_2$ electrode within a stability potential window between −1.0 and 0.1 V (versus SCE) at a scan rate of 5 mV s^{-1}. Such lower voltage limit without noticeable hydrogen evolution and good reversibility of $Ru_{0.36}V_{0.64}O_2$ electrode indicate that the material is very suitable for a negative electrode in a hybrid EC system. The shape of the CV of $Ru_{0.36}V_{0.64}O_2$ electrode is pseudorectangular, suggestive of fast and reversible faradic redox reactions of $Ru_{0.36}V_{0.64}O_2$. It is well known that the vanadium oxides can react with KOH and subsequently dissolved in the alkaline electrolyte solution. However, the $Ru_{0.36}V_{0.64}O_2$ electrode can be cycled several hundred times without significant noticeable modification of the CV within the electrochemical window of −1.0 to 0.1 V (versus SCE) in 1 M KOH, which indicates the formation of Ru–V solid solution [19] and the good stability of $Ru_{0.36}V_{0.64}O_2$ electrode in the KOH electrolyte. Also, due to the addition of V into the ruthenium oxide, the electrochemical window of $Ru_{0.36}V_{0.64}O_2$ electrode turns much larger from much less than 1.0 V [11] to 1.1 V. Therefore, the introduction of V species is believed to not only increase the utilization of Ru species but also enhance the electrochemical stability although pseudocapacitance of $Ru_{0.36}V_{0.64}O_2$ should be mainly contributed by the electroactive oxyruthenium species (i.e., RuO_2).

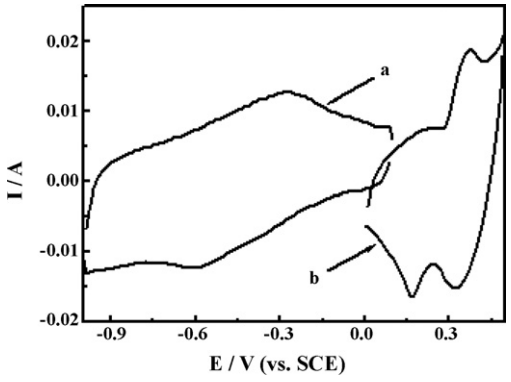

Fig. 2. CV curves of (a) $Ru_{0.36}V_{0.64}O_2$ and (b) NiO electrodes at 5 mV s^{-1}.

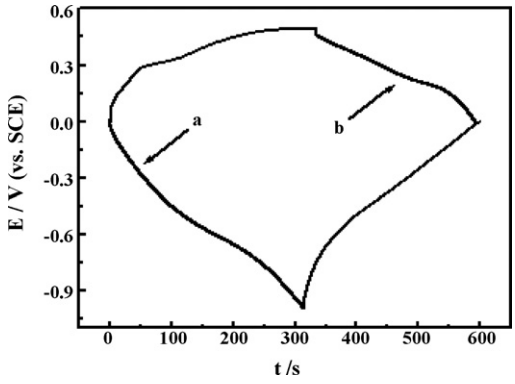

Fig. 3. Charge–discharge curves of (a) $Ru_{0.36}V_{0.64}O_2$ and (b) NiO electrodes at 6 mA cm^{-2}.

And the *E–i* response of NiO without noticeable oxygen evolution, within an electrochemical window of 0.0–0.5 V (versus SCE) at 5 mV s^{-1}, is also shown in Fig. 2b. The potential window of the NiO electrode is shift toward positive value compared to the $Ru_{0.36}V_{0.64}O_2$ electrode. The CV of the NiO electrode is characterized by a set of reduction and oxidation waves centered at 0.17 and 0.37 V versus SCE, respectively, which is distinguished from that of the electric double-layer capacitance in which case it is normally close to an ideal rectangular shape, indicating that the capacity mainly results from the pseudocapacitance. The redox waves are associated with a reversible redox interconversion between Ni(II) and Ni(III). Moreover, the overlapping of their useful electrochemical windows of two CV curves, in Fig. 2a and b, indicates the feasibility of designing a hybrid capacitor just by correctly balancing the weight of active materials in both the electrodes.

The typical galvanostatic charge–discharge curves at 6 mA cm^{-2}, of the NiO electrode within a potential window of 0.0–0.5 V (versus SCE) and $Ru_{0.36}V_{0.64}O_2$ electrode within an electrochemical window of −1.0 to 0.0 V (versus SCE), are shown in Fig. 3. Linear variation of the voltage is not observed for both the positive and negative electrodes in Fig. 3a and b, which is attributed to the potential dependent nature of faradic redox reactions and in well agreement with the CV curves analysis. In addition, the SCs delivered by $Ru_{0.36}V_{0.64}O_2$ and NiO are about 342 and 310 F g^{-1}, respectively, which are evaluated from the typical galvanostatic charge–discharge curves shown in Fig. 3a and b.

3.3. Electrochemical performance of the hybrid EC based on NiO and $Ru_{0.36}V_{0.64}O_2$ electrodes

Cyclic voltammmetry (CV) at various sweep rates was used to determine the electrochemical characteristics of the hybrid EC in aqueous media with 1 M KOH as a supporting electrolyte. The typical CV response of the asymmetric EC, in Fig. 4, shows that the hybrid EC owns good electrochemical capacitive

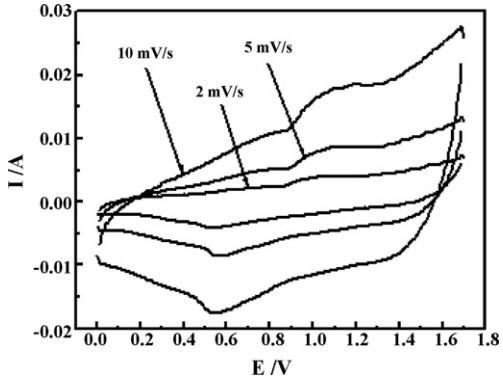

Fig. 4. CV curves of the asymmetric EC based on $Ru_{0.36}V_{0.64}O_2$ and NiO electrodes at various scan rates as indicated.

behavior. And moreover, the current–potential response is potentially dependent in contrast to the potential-independent current response of an electrochemical capacitor based on non-faradic process. And the SCs of the hybrid system can be calculated from the CV curves according to the following equation:

$$C_m = \frac{i}{mv} \tag{1}$$

where m is the total mass of active materials in both the two electrodes, v the potential sweep rate, and i is the even current response defined by $i = \left(\int_{V_a}^{V_c} i(v)\mathrm{d}v\right)/(V_c - V_a)$, where V_a and V_c represent the lowest and highest voltage, respectively. i is obtained through integrating the area of the curves in Fig. 4. The SCs are ca. 71, 73, 76 F g^{-1}, respectively, with the scan rates of 10, 5, 2 mV s^{-1}, respectively.

Galvanostatic constant current charge/discharge measurements at different current densities were applied to evaluate the electrochemical properties and to quantify the SC of the hybrid EC in 1 M KOH electrolyte. Fig. 5 shows the typical galvanostatic charge–discharge curves of the hybrid EC between 0.0 and 1.7 V at different current densities. As seen from Fig. 5, the E–t responses behave as triangular shape during the charge–discharge processes, suggestive of a good electrochemical performance of the hybrid EC. And it is worthy of being noted that the charge/discharge curves all display a slop

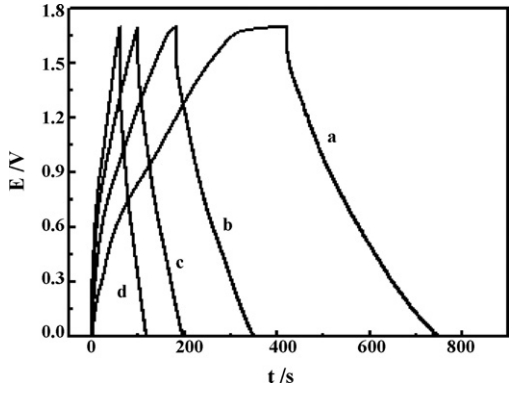

Fig. 5. Typical charge–discharge curves of the hybrid EC at different current densities: (a) 7.5 mA cm^{-2}; (b) 12.5 mA cm^{-2}; (c) 17.5 mA cm^{-2}; (d) 25.0 mA cm^{-2}.

variation of time dependence of the potential and are not perfectly linear as is the case of activated carbon-based capacitors [2], indicative a typical pseudocapacitance behavior resulting from the electrochemical adsorption/absorption or redox reactions at interfaces between electrodes and electrolyte. Moreover, the discharge profiles all contain two parts: a resistive component arising from the sudden voltage drops (linear portion parallel to y-axis) representing the voltage change due to the internal resistance and a capacitive component (curve portion) related to the voltage change due to change in energy within the capacitance on all curves in Fig. 5. In addition, the sudden potential drops, obeying the ohmic law, become less with the decrease of the charge–discharge current density.

And the SC of the asymmetric hybrid EC could be calculated as follows:

$$C_m = \frac{C}{m} = \frac{It}{\Delta V(m_p + m_n)} \tag{2}$$

where I, t, ΔV, respectively, indicate the constant current that is applied, the discharge time, the efficient electrochemical window, and the m_p, m_n represent the mass loadings of positive and negative electrode material, respectively. The typical SCs of the hybrid system are shown in Table 1, from the results summarized in Table 1, it is clear that the SCs decrease gradually with increasing discharge current density. The reasons for the loss in the SCs at higher charge/discharge current density could be mainly from two aspects: (a) the large IR drop at a large discharge current density that leads to the small SCs; (b) activation polarization and concentration polarization at higher charge/discharge current that results the low utilization of the electroactive materials.

And the specific energy density (E) of the hybrid EC can be calculated by means of the following Eq. (3) and the typical results are shown in Table 1.

$$E = C_m \int V\,\mathrm{d}v = \frac{1}{2}C_m(\Delta V)^2 \tag{3}$$

It is well established that a hybrid supercapacitor can be considered as two capacitors in series [17]. So the average SC of the hybrid EC can be obtained from the following equation:

$$C_{average} = \frac{C_{NiO}m_{NiO}C_{Ru_{0.36}V_{0.64}O_2}m_{Ru_{0.36}V_{0.64}O_2}}{m_{NiO} + m_{Ru_{0.36}V_{0.64}O_2}} \tag{4}$$

where C_{NiO} and $C_{Ru_{0.36}V_{0.64}O_2}$ are the SCs of NiO and $Ru_{0.36}V_{0.64}O_2$, respectively; and m_{NiO} and $m_{Ru_{0.36}V_{0.64}O_2}$ are the weights of NiO and $Ru_{0.36}V_{0.64}O_2$, respectively. Subsequently, the calculation leads to a value of ca. 111 F g^{-1} of the total active material, which is basically in agreement with the values determined from the galvanostatic constant current charge/discharge tests.

Table 1
The SCs and specific energy density (E) of the hybrid EC based on the curves in Fig. 5

Current density (mA cm^{-2})	7.5	12.5	17.5	25.0
C_m (F g^{-1})	102.6	83.8	66.9	57.4
E (Wh kg^{-1})	41.2	33.6	26.9	23.0

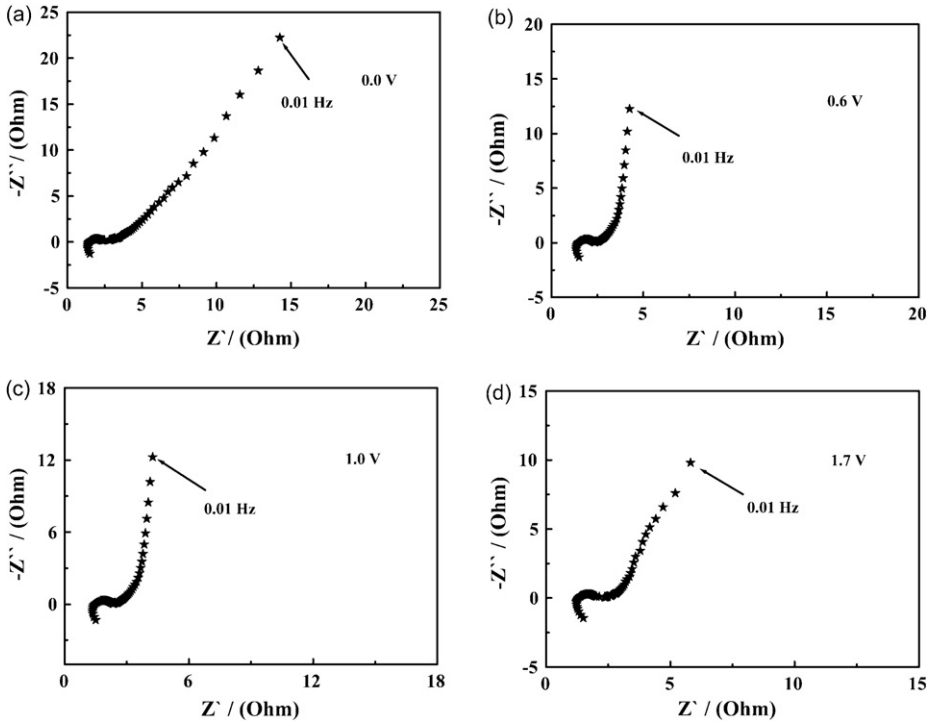

Fig. 6. Nyquist plots of the hybid EC at different applied potentials: (a) 0.0 V; (b) 0.6 V; (c) 1.0 V; (d) 1.7 V.

Electrochemical impedance spectroscopy (EIS) analysis is a very powerful tool to characterize the electrochemical process of an EC. To better evaluate the performance of the hybrid EC, the electrochemical impedance measurements at different applied potentials between 0.0 and 1.7 V (the frequency range set from 100 K to 0.01 Hz with 5 mV amplitude) were carried out, and the typical complex plane plots were shown in Fig. 6.

Three distinct regions, dependent on the frequency range, are shown in Fig. 6(a–d), From the points intersecting the real axis in the range of high frequency, it can be seen that the values of the internal resistance (R_i) of the hybrid EC at all the applied potentials are nearly the same and estimated as little as ca. 1.5 Ω. In the high-medium frequency region, from the semi-circles observed for all the plots, the charge-transfer resistances (R_{ct}) related to charge-transfer process on the surfaces of the electroactive materials are estimated the same as ca. 0.3 Ω at various applied potentials. And it is clear that, in the low frequency region, the slope of all the impedance plots increases and almost tends to a vertical asymptote, indicative of the good electrochemical capacitance performance of the hybrid EC within the applied voltage range from 0.0 to 1.7 V, which is well consistent with the analysis of the CV tests in Fig. 4.

Also, the SCs of the hybrid EC at different applied potentials can be evaluated from EIS test according to the following equation:

$$C_m = \frac{1}{(m_p + m_n) \times (j\omega Z'')} \quad (5)$$

where C_m is the SC of the hybrid EC; $j = -1$; $\omega = 2\pi f$; f the frequency (0.01 Hz); Z'' the imaginary part of the impedance test, m_p and m_n are the mass of the active material in positive and negative electrodes, respectively. And the SCs of the asymmetric hybrid EC at various applied potentials are summarized in Table 2 and the change trend of SC with the potential basically is in agreement with the results of CV tests in Fig. 4.

Table 2
The SCs of the hybrid EC at different applied potentials evaluated from EIS test

Potential (V)	0.0	0.6	1.0	1.7
C_m (F g^{-1})	53.8	62.8	87.4	98.6

In order to highlight the electrochemical performance of the hybrid EC based on NiO and $Ru_{0.36}V_{0.64}O_2$ electrodes, the Ragone plot relating power density to achievable energy density of the asymmetric EC is also demonstrated in Fig. 7.

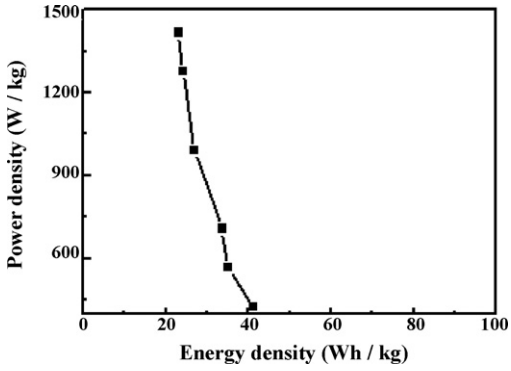

Fig. 7. Ragone plot relating power density to achievable energy density of the hybrid EC.

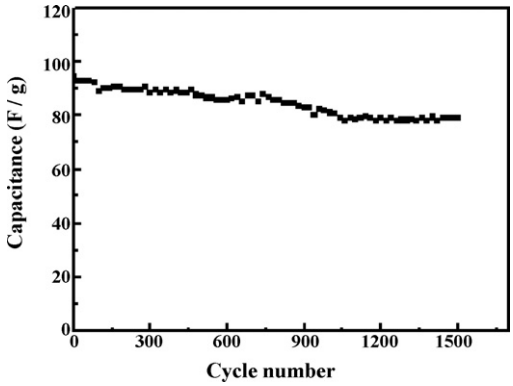

Fig. 8. Charge–discharge cycle of the hybrid EC at 10 mA cm^{-2}.

The specific power density (P) of the hybrid EC can be calculated from the following equation:

$$P = \frac{I\Delta V}{2(m_p + m_n)} \quad (6)$$

where I is the constant charge–discharge current density, ΔV the potential range of the hybrid EC, m_p and m_n are the mass of active material in the positive and negative electrodes, respectively. It is evident that the specific power density of 1416.7 W kg^{-1} and specific energy density of 23.0 Wh kg^{-1} are obtained at a current density of 25.0 mA cm^{-2}.

The cyclability of the hybrid EC was performed by charge–discharge at a current density of 10 mA cm^{-2} within a voltage range of 0.0 and 1.7 V in 1 M KOH electrolyte. Fig. 8 shows the variation of SC of the hybrid EC as a function of cycle number. As shown in Fig. 8, the capacitance of the hybrid EC decreases with the growth of the cycle number. After continuous 1500 cycles, the capacitance value remains ca. 83.5% of that of the first cycle. The attenuation of the capacitance just for 16.5% suggests the good cyclic stability of the hybrid EC, which is significant for the practical application. It is only when the range of electroactivity and electrochemical stability of both the electrodes is totally taken into account that the origin of the capacity fade can be found. The overcharging and/or overdischarging of the hybrid EC could result in a decrease in the active materials available for further cycling and subsequently to a capacitance loss. Also, it is out of question that the electrochemical reversibility of NiO and $Ru_{0.36}V_{0.64}O_2$ electrodes should be responsible for the capacitance fade. And specific reasons of the capacitance fade of the hybrid EC will be detailed in our forthcoming study. Moreover, the issue of gas evolution remains, and should be paid more attention to and be carefully and further investigated although there is no visible gas evolution happening during cycling.

When the constant current is used for charging and discharging processes, an important parameter, coulombic efficiency (η), can be evaluated from the following equation:

$$\eta = \frac{t_D}{t_C} \times 100\% \quad (7)$$

where t_D and t_C are the time for galvanostatic discharging and charging, respectively. The data evaluated from the charge/discharge curves of the hybrid EC at different cycle is shown in Table 3. It is clear that the coulombic efficiency increases with the growth of cycle number. After 1500 cycles without relaxation between cycles, the coulombic efficiency approaches 98.1%.

Table 3
The capacitance and coulombic efficiency characters evaluated from the charge/discharge tests between 0.0 and 1.7 V

Cycle number	SC (F g^{-1}) at 10 mA cm^{-2}	Coulombic efficiency η (%)
First cycle	94.5	96.2
750th cycle	86.1	97.5
1500th cycle	78.9	98.1

4. Conclusions

In summary, negative material $Ru_{0.36}V_{0.64}O_2$ and positive material NiO have been synthesized and applied to assemble an asymmetry hybrid EC. Electrochemical tests revealed that $Ru_{0.36}V_{0.64}O_2$ had good electrochemical performance in the potential window from −1.0 to 0.1 V (versus SCE) and the NiO within electrochemical window of 0–0.5 V (versus SCE) in 1 M KOH electrolyte. The hybrid EC based on $Ru_{0.36}V_{0.64}O_2$ and NiO electrodes exhibited good electrochemical capacitance behavior within the potential range from 0.0 to 1.7 V. The specific energy density reached 41.2 Wh kg^{-1} at specific power density of 425 W kg^{-1} and decreased to 23.0 Wh kg^{-1} when the specific power density was up to 1416.7 W kg^{-1}. The hybrid EC also demonstrated a good cycling performance with an attenuation of capacitance of ca. 16.5% over 1500 cycle numbers.

Acknowledgements

This work was supported by National Natural Science Foundation of China (No. 20403014, No. 20633040) and Natural Science Foundation of Jiangsu Province (BK2006196).

References

[1] K.H. An, W.S. Kim, Adv. Funct. Mater. 11 (2001) 387.
[2] B.E. Conway, Electrochemical Supercapacitors: Scientific Fundamentals and Technological Applications, Kluwer Academic Publishers/Plenum Press, New York, 1999 (Chapter 20).
[3] S.T. Mayer, R.W. Pekela, J.L. Kaschmitter, J. Electrochem. Soc. 14 (1993) 446.
[4] C.C. Hu, J.Y. Lin, Electrochem. Acta 47 (2002) 4055.
[5] C.C. Hu, W.Y. Li, J.Y. Lin, J. Power Sources 137 (2004) 152.
[6] J.P. Zheng, P.J. Cygan, T.R. Jow, J. Electrochem. Soc. 142 (1995) 2699.
[7] Y. Takasu, Y. Murakami, Electrochim. Acta 45 (2000) 4135.
[8] S. Trasatti, Electrochim. Acta 36 (1991) 225.
[9] C. Angeliretta, S. Trasatti, L.D. Atanasoska, R.T. Atanasoski, J. Electrochem. Soc. 214 (1986) 535.
[10] F.B. Zhang, Y.K. Zhou, H.L. Li, Mater. Chem. Phys. 83 (2004) 260.
[11] Y.G. Wang, Z.D. Wang, Y.Y. X, Electrochim. Acta 50 (2005) 5641.
[12] J.H. Park, O.O. Park, J. Power Sources 111 (2002) 185.
[13] A.D. Pasquier, I. Plitz, J. Gural, S. Menocal, G. Amatucci, J. Power Sources 113 (2003) 62.
[14] T. Brousse, M. Toupin, D. Belanger, J. Electrochem. Soc. 151 (2004) 614.
[15] C. Arbizzani, M. Mastragostino, F. Soavi, J. Power Sources 100 (2001) 164.
[16] T. Brouse, D. Belanger, Electrochem. Solid-State Lett. 6 (11) (2003) A244.

[17] C.Z. Yuan, X.G. Zhang, Q.F. Wu, B. Gao, Solid State Ionics 177 (2006) 1237.
[18] G.T. Chandrappa, N. Steunou, S. Cassaignon, C. Bauvais, J. Livage, Catal. Today 78 (2003) 85.
[19] W. Sugimoto, T. Shibutani, Y. Murakami, Y. Takasu, Electrochem. Solid-State Lett. 5 (7) (2002) A170.
[20] K. Yokoshima, T. Shibutani, M. Hirota, W. Sugimoto, Y. Murakami, Y. Takasu, J. Power Sources 160 (2006) 1480.